Advances in Environmental Technology

Evaluation of LaBO$_3$ (B=Mn, Cr, Mn$_{0.5}$Cr$_{0.5}$) perovskites in catalytic oxidation of trichloroethylene

Samereh Eskandarya, Sarah Maghsoodi[*], **Amirhossein Shahbazi Kootenaei**

Department of Chemical Engineering, Mahshahr Branch, Islamic Azad University, Mahshahr, Iran.

ARTICLE INFO

ABSTRACT

In this study, La–Mn–Cr perovskite-type catalysts were synthesized as LaMnO$_3$, LaCrO$_3$, and LaMn$_{0.5}$Cr$_{0.5}$O$_3$ by a microwave-assisted gel-combustion method. They were then calcined at 600ºC for 5h in air. X-ray diffraction (XRD) analysis indicated that the crystalline perovskite phase is the dominant phase formed in all the synthesized samples. The scanning electron microscopy (SEM) analysis showed that the perovskites have a full spongy and porous structure. The specific surface area (BET) analysis showed a specific surface area of about 12.4-26.8 m^2/g, and the highest specific surface area belonged to the LaMn$_{0.5}$Cr$_{0.5}$O$_3$ perovskite. Moreover, the highest oxygen mobility revealed by the temperature-programmed desorption of oxygen (O$_2$–TPD) analysis was related to the LaMn$_{0.5}$Cr$_{0.5}$O$_3$ sample. The catalytic activity of the synthesized perovskites in catalytic oxidation of 1000 ppm trichloroethylene (TCE) in air was investigated at different temperatures. The substituted perovskite (LaMn$_{0.5}$Cr$_{0.5}$O$_3$) with the highest BET specific surface area and the highest oxygen mobility yielded the best catalytic performance among the probed perovskites.

1. Introduction

The air pollution, especially in industrial cities, produced by toxic and dangerous gases is one of the pressing consequences of the industrialization of urban communities. It can lead to problems such as birth defects, economic loss, premature aging, depreciation of materials used in buildings, acid rain, increased corrosion of metals, and many other consequences. Volatile organic compounds (VOCs) are recognized as one of the leading causes of air pollution with their high concentrations, mostly in industrial and urban areas. VOCs are directly related to air quality and significantly contribute to the formation of smog. Trichloroethylene (TCE) is one of the most common chlorinated volatile organic compounds widely employed in many industries such as electronics; it is also used as a solvent for many organic materials, metallic surfaces, adhesives, and in dry cleaners. In addition to its harmful effects on general health, this compound damages the ozone layer as well, due to its long-term storage and accumulation in the environment [1,2]. Catalytic oxidation is one of the most commonly used techniques for control of the emissions of volatile organic compounds. Perovskite-type (ABO$_3$) catalysts have shown promising results in catalytic oxidation of VOCs [3]. Catalytic properties of perovskites for the oxidation of pollutants strongly depend on the nature of B–site cations [4,5]. Sinquin et al. [6] reported that LaMnO$_{3+\delta}$ is more active and stable than LaCoO$_3$ in the destruction of chlorinated compounds. In the comparative study of the activity of ABO$_3$ perovskites, including La, Y, Nd, and Gd in A–site as well as Co, Fe and Cr in B–site, despite the less specific surface area, Cr containing perovskites possessed superior catalytic activity in oxidation of 1, 2–dichlorobenzene [7]. Although the stoichiometry state has often been observed in the structure of most perovskites, there are still perovskites with non-stoichiometric defects. The formation of A and B vacancies in a sample with an A/B ratio of 1 is reported [8].
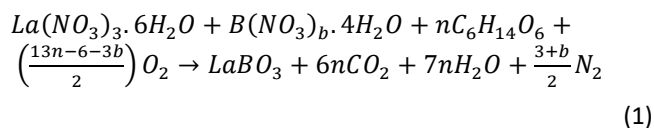
In our previous work [9], we have shown that the increased ratio of Mn/La and Co/La in the lanthanum manganite and lanthanum cobaltite perovskite catalysts up to 20% compared to the stoichiometric one led to the improvement of the BET surface area, oxygen mobility, and consequently catalytic performance. Another distinct way for the generation of structural defect is by the partial substitution of A and B-site cations that results in cation vacancies (with positive holes) and/ or oxide ions vacancies [10]. Creating such network defects directly or indirectly affects the catalyst properties of perovskites. Usually, the optimum value of substitution that leads to the highest catalytic activity depends on the oxidized reagent. By mixing two catalytically active cations in the B-site, a consistent and powerful effect can be achieved; one cation promotes the adsorption of the reagent, and the other component creates a high reactivity of lattice oxygen. For instance, the substitution of Mn with Cu in $LaMnO_3$ ($LaMn_{0.6}Cu_{0.4}O_3$) or Ni in $LaMnO_3$ ($LaMn_{0.9}Ni_{0.1}O_3$) enhances the activity for CO and ethanol oxidation, respectively [11,12]. Moreover, $LaMn_{0.9}Fe_{0.1}O_3$ has a higher catalytic activity than $LaMnO_3$ and $LaFeO_3$ perovskites for the oxidation of methane [13]. This paper investigated the preparation of an efficient perovskite for the oxidative removal of trichloroethylene. Therefore, the activity of synthesized $LaMnO_3$, $LaCrO_3$, and the substituted perovskite ($LaMn_{0.5}Cr_{0.5}O_3$) in the catalytic aerobic oxidation of 1000 mg/l trichloroethylene at different temperatures was investigated and compared. The perovskites were synthesized by the gel-combustion method that Maghsoodi et al. [14] and Prado et al. [15] introduced; this method with the aid of microwave irradiation is a fast, economical, environmentally friendly, and suitable method for perovskite synthesis.

2. Materials and methods

2.1. Synthesis of catalysts

The $LaMnO_3$ and $LaCrO_3$ perovskites, as well as the substituted one ($LaMn_{0.5}Cr_{0.5}O_3$), were synthesized by the microwave-assisted gel-combustion method. In the synthesis, lanthanum nitrate (La $(NO_3)_3.6H_2O$), manganese nitrate ($Mn(NO_3)_2.4H_2O$), and chromium nitrate ($Cr(NO_3)_2.4H_2O$) were used as oxidizers and sorbitol ($C_6H_{14}O_6$) as the organic fuel. All these materials were purchased from the Merck Company. The stoichiometric ratio of fuel to oxidizer (1:1) was applied in all of the synthesis. A calculated amount of starting materials were poured into a crucible, and two cc of deionized water was added to the mixture. The mixing operation was conducted on a hot plate at 140°C for 15 minutes, so a perfectly homogeneous gel-like blend was obtained. Then the resulting gel was placed in an 850 watts microwave for the combustion process. In less than 25 seconds, the combustion process was finished while releasing a large quantity of gases. The resulting product from the combustion process, which had a spongy form, was calcined

at 600°C for 5 h in air atmosphere. Finally, the samples from the calcination were sieved at the range of 0.152–0.251 mm (60–100 mesh size). Equation 1 indicates the combustion synthesis reactions for the synthesis of $LaMnO_3$, $LaCrO_3$ and $LaMn_{0.5}Cr_{0.5}O_3$ perovskites, where B is the Mn, Cr, or 50%-50% Mn–Cr.

$$La(NO_3)_3.6H_2O + B(NO_3)_b.4H_2O + nC_6H_{14}O_6 + \left(\frac{13n-6-3b}{2}\right)O_2 \rightarrow LaBO_3 + 6nCO_2 + 7nH_2O + \frac{3+b}{2}N_2$$

(1)

All the precursors were weighed and used according to the stoichiometric ratios of Equation 1.

2.2. Characterization of the catalysts

2.2.1. XRD analysis

X-ray powder diffraction (XRD) analyses were performed by a PW 1800 diffractometer made by the Philips Company using Cu-Kα radiation. The diffraction intensity for all samples was measured within the range of $20° < 2θ < 70°$ with the step size of $0.03°$ and a count time of 2 seconds per each step. The resulting XRD patterns were analyzed by comparison with the data in the Joint Committee on Powder Diffraction Standards (JCPDS). The average size of the synthesized crystals was calculated by the Debye-Scherrer equation (Eq. 2) [5].

$$d_{XRD} = \frac{k\lambda}{\beta \cos \theta}$$

(2)

In this equation, d_{XRD} is the crystallite size in nanometers, k is a constant equal to 0.89, λ is the wavelength of the used x-ray, β is the index peak width at half peak height, and θ is the angle between the diffracted and input rays.

2.2.2. BET Analysis

The specific surface areas of the synthesized catalysts were measured by BET analysis using a Nova Station manufactured by the Quantachrome NovaWin2 Company. Prior to BET analysis, the samples were degassed at 300°C for 2 h. Then, the BET surface area measurement was determined using a single-point method at the liquid nitrogen temperature, which was obtained by the adsorption and desorption isotherms of nitrogen.

2.2.3. SEM analysis

The morphology and particle size of the catalysts were determined by scanning electron microscope (SEM) analysis using a TESCAN Vega apparatus.

2.2.4. O₂-TPD analysis

The O_2-temperature programmed desorption (O_2–TPD) of the synthesized catalysts were determined by a multifunctional device manufactured by the Quantachrome Company, model CHEMBET–3000. First, the sample was preheated at room temperature to 300°C under a 20 sccm

(standard cubic centimeters per minute) oxygen flow and kept at this temperature
for 1h. Then, the temperature of the sample was cooled to room temperature under the same flow of oxygen. After ending this process, oxygen was adsorbed on the catalyst surface, and the catalyst was fully oxidized. Then, the oxygen flow was switched off, and a helium flow (20 sccm) was passed through the catalyst for 30 minutes at room temperature to clean the physically bounded oxygen on the catalyst surface. Finally, the temperature of the sample was increased to 1000°C under helium flow at the rate of 10°C/min, and desorption of the oxygen from the surface and lattice was monitored by a TCD.

2.3. Evaluation of catalytic activity

The system was designed for a catalytic activity test; its simplified scheme is shown in Figure 1. The dry air and the VOC were directed to the reactor through mass flow controllers that provided the desired rate of gas, which was kept constant throughout the experiment. It is noteworthy that before performing the tests, each mass flow controller was calibrated for the relevant gas. A quartz reactor with a length of 50 cm, an inner diameter of 7 mm, and an outer diameter of 9 mm was used. The catalyst sample was placed at the reactor core on a piece of ceramic wool. An electric furnace was used for heating the reactor with a temperature controller adjusting the furnace temperature. A K-type thermocouple, which was connected to a temperature controller, was placed in the furnace near the catalyst bed in the reactor.
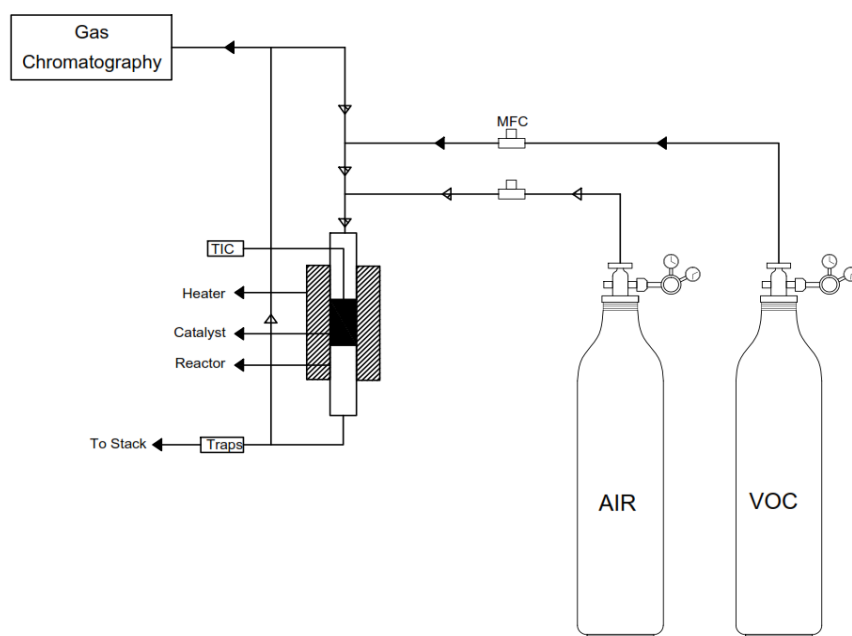

Fig. 1. The laboratory system designed to investigate the activity of catalytic oxidation.

In each experiment, 0.1 g of the catalyst sample was utilized for the evaluation of the activity of the catalysts for the oxidation of 1000 mg/l trichloroethylene. First, the catalyst was heated to 600°C under a flow of air (30 sccm) with a heating rate of 10°C/min starting from room temperature. The reaction was conducted at various temperatures from 600°C down to room temperature. In each step, a 30 sccm flow of 1000 mg/l trichloroethylene in air was passed through the catalyst bed. The exhaust gases from the reactor were analyzed by an Agilent 6895 N gas chromatograph, equipped with a capillary column CP-Sil 52 CB. After taking the effluent sample, cooling the reactor was conducted in airflow until the next desired temperature was reached. The conversion of the pollutant was calculated using the difference between the concentrations of its input and output (Eq. 3).

$$Conversion\ (\%) = \frac{[VOC]_{in} - [VOC]_{out}}{[VOC]_{in}} \times 100 \qquad (3)$$

3. Results and discussion

3.1. Catalysts characterizations

3.1.1. XRD analysis

Figure 2 presents the XRD spectra of the synthesized catalysts: LaMnO$_3$, LaCrO$_3$, and LaMn$_{0.5}$Cr$_{0.5}$O$_3$. The resulting spectra show the formation of the perovskite structure in all the synthesized samples. In Figure 2a, all the observed peaks can be attributed to LaMnO$_3$ perovskite (JCPDS 32-0484) [3]. The presence of other possible impurities such as oxides of manganese or lanthanum is denied. In regard to the LaCrO$_3$ perovskite in Figure 2b, the peaks of impurities such as La$_2$O$_3$ and Cr$_2$O$_3$, whose formation is mentioned in

studies by other researchers [16,17], is not observed and the perovskite phase is the dominant observed phase. In Figure 2c, concerning $LaMn_{0.5}Cr_{0.5}O_3$, all the peaks belong to the perovskite, and the diffractogram indicates the formation of perovskite as a single phase, confirming the insertion of the Cr in $LaMnO_3$ perovskite structure.

As can be noted in Figure 2, a reduction of the XRD peak intensities of the $LaMn_{0.5}Cr_{0.5}O_3$ sample was observed. The broadening and shifts in the XRD peak could be caused by either a reduction in the grain size (Scherrer broadening) and/or a non-uniform strain (microstrain). The lower intensities of the XRD patterns after the substitution of different elements have been reported in the literature. For example, the Perovskite-like phase, with a lower pattern intensity, was observed after the substitution of Cu^{2+} and Ni^{2+} cations in the $LaFeO_3$ perovskite framework [18]. In another report, a series of $LaBO_3$ (B = Cr, Co, Ni, Mn) and $La_{0.9}K_{0.1}MnO_{3+\delta}$ perovskites were prepared and tested as catalysts in the combustion of methyl ethyl ketone. The incorporation of potassium gave rise to a slight drop in peak intensity [19]. The average size of the synthesized crystals (d_{XRD}) was calculated by the Scherrer equation (Eq. 2) and is displayed in Table 1. As may be noticed in the presented results, the average sizes of the synthesized crystals were in the range of 16 to 30 nm. In similar studies that used different synthesis methods, the crystalline particle sizes for $LaMnO_3$ were found to be 25 nm [15] and 20-30 nm [20]; those for $LaCrO_3$ were about 1 μm [15] and 78.5 μm [19]. According to the calculations performed in this study and the aforementioned studies, the size of the synthesized crystals was relatively comparable. That could be attributed to the synthesis method and the calcination temperature.
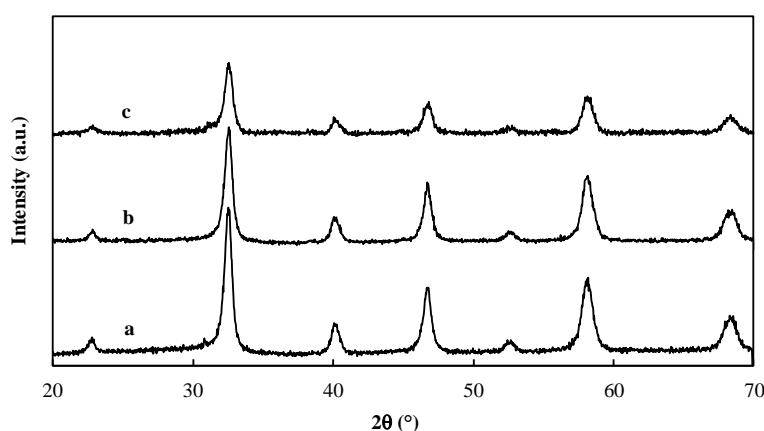

Fig. 2. XRD patterns of the perovskites (a) $LaMnO_3$, (b) $LaCrO_3$ and (c) $LaMn_{0.5}Cr_{0.5}O_3$.

3.1.2. SEM analysis

The SEM images of the $LaMnO_3$, $LaCrO_3$, and $LaMn_{0.5}Cr_{0.5}O_3$ catalysts that were synthesized with the gel-combustion method are shown in Figures 3a, b and c. These images show that all the synthesized perovskites have a fully spongy and porous structure. As a large amount of gas was released during the synthesis of the catalysts by the gel-combustion method under microwave irradiation, a porous structure with a spongy morphology could be expected [14].
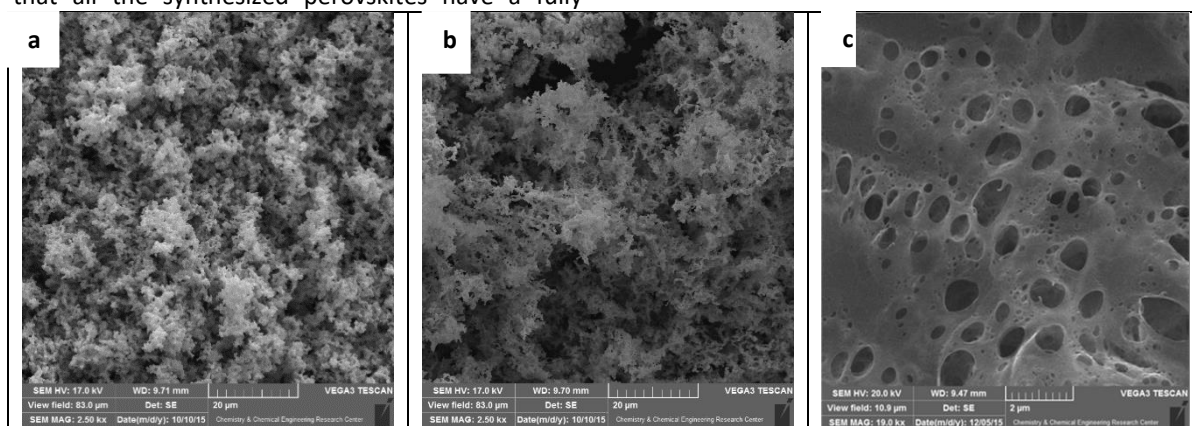

Fig. 3. SEM images of catalysts (a) $LaMnO_3$, (b) $LaCrO_3$ and (c) $LaMn_{0.5}Cr_{0.5}O_3$ synthesized by the gel-combustion method.

3.1.3. BET analysis

The results of the BET specific surface area of the probed catalysts are exhibited in Table 1. The specific surface area of $LaMnO_3$, $LaCrO_3$, and $LaMn_{0.5}Cr_{0.5}O_3$ were about 16.1, 12.4, and 26.8 m^2/g, respectively. The maximum specific surface area was associated with the $LaMn_{0.5}Cr_{0.5}O_3$ perovskite. In other words, the simultaneous and equal replacement of the two cations, namely chromium and manganese, into perovskite structure led to an increase in specific surface area for more than 2-fold and 1.5-fold compared to $LaCrO_3$ and $LaMnO_3$, respectively. This has previously been reported for the catalyst $LaMn_{0.6}Cu_{0.4}O_3$, whose specific surface area is higher than $LaMnO_3$ and $LaCuO_3$ [13]. Perovskites generally have a low specific surface area, and their particle size and specific surface area depend on the synthesis method and calcination temperature. For instance, other researchers reported a specific surface area of about 6 m^2/g for $LaCrO_3$ and $LaMnO_3$ [19]. Moreover, for the substituted perovskites $LaCr_{0.5}Co_{0.5}O_3$ and $LaMn_{0.5}Co_{0.5}O_3$ that were synthesized by the sol–gel method, the measured specific surface area was 11.3 and 12.6 m^2/g, respectively [21].

Table 1. Average crystalline size (d_{XRD}), specific surface area (S_{BET}), T_{50} (°C), and T_{90} (°C) of the synthesized catalysts for oxidation of 1000 mg/l trichloroethylene in air.

Catalyst	d_{XRD} (nm)	S_{BET} (m^2/g)	T_{50} (°C)	T_{90} (°C)
$LaMnO_3$	16.8	16.1	400	500
$LaCrO_3$	20.3	12.4	350	480
$LaMn_{0.5}Cr_{0.5}O_3$	30.1	26.8	300	380

3.1.4. O₂-TPD analysis

The acquired oxygen adsorption and desorption profiles of the synthesized perovskites (O₂-TPD) are shown in Figure. 4a. Two characteristic peaks are discernible in the O₂-TPD spectra of the studied samples: (1) the first peak is located in the range of 300-700°C that is related to α oxygen; and (2) the second peak is located at temperatures higher than 700°C, which is related to β oxygen. The first peak is related to the oxygen absorbed in the anionic vacancy at the surface, which is more mobile. The second peak is attributed to the oxygen species with a stronger bond and is usually released from the perovskite lattice bulk [22].
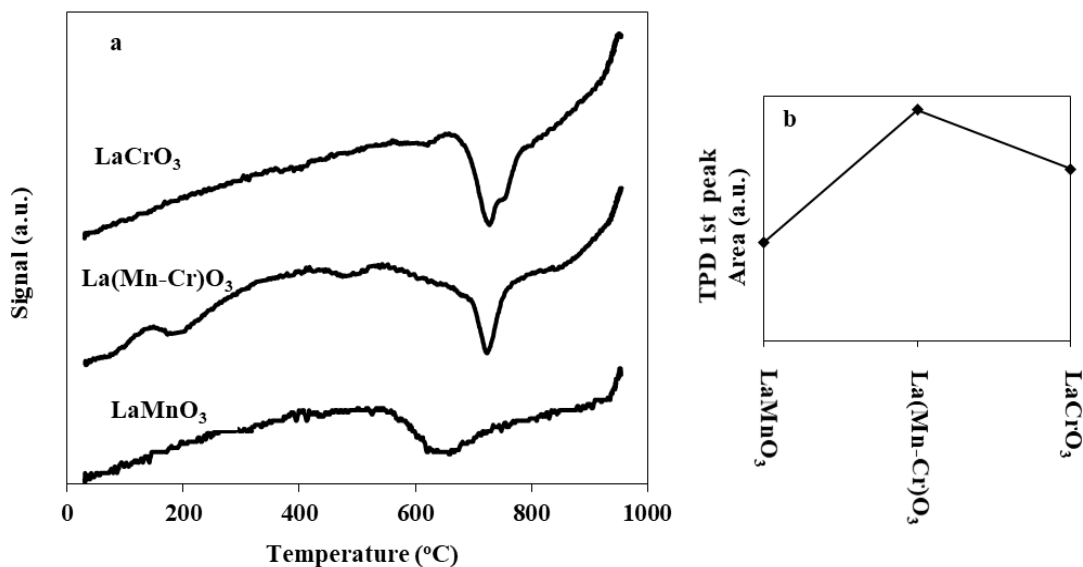

Fig. 4. (a) O₂-TPD spectra; and (b) area of the first peak (T=300-700 °C) for $LaMnO_3$, $LaCrO_3$, and $LaMn_{0.5}Cr_{0.5}O_3$.

Thus, the β oxygen as compared to the α oxygen requires higher temperatures for disposal. In other words, the α and β oxygen originates from the surface and bulk, respectively. The amount of oxygen released in the second peak (>700°C) generally does not play an important role in the oxidation of trichloroethylene, since this compound is totally converted at temperatures below 600°C. Thus, the area of the first peak, which plays an important role in catalytic activity, has been determined for the synthesized perovskites and is presented in Figure. 4b. It is noted that the order of oxygen mobility in the investigated catalysts is $LaMn_{0.5}Cr_{0.5}O_3$ > $LaCrO_3$ > $LaMnO_3$. Thus, we can conclude that chromium-containing perovskites have higher oxygen mobility in comparison with manganese-containing ones. Moreover, the substituted perovskite ($LaMn_{0.5}Cr_{0.5}O_3$) possess higher oxygen mobility compared to the unsubstituted ones,

3.2. Evaluation of catalytic activity for oxidation of trichloroethylene

The measured oxidation activity of the synthesized catalysts $LaMnO_3$, $LaCrO_3$, and $LaMn_{0.5}Cr_{0.5}O_3$ for the oxidation of

1000 mg/l trichloroethylene in the air is shown in Figure. 5. Trichloroethylene is one of the most common chlorinated VOCs. The presence of a double bond beside the chlorine atom enhances the resistance of trichloroethylene ($CHCl=CCl_2$) against dehydrochlorination. As reported, the degradation of TCE requires high temperatures of around 500°C using Pt/Al_2O_3 catalysts [23]. The values of T_{50} and T_{90} are presented in Table 1. These temperatures (T_{50} and T_{90}) are defined as temperatures required to convert 50% and 90% of trichloroethylene, respectively.

Although $LaCrO_3$ has a smaller specific surface area than $LaMnO_3$, a higher performance is observed for this sample in the aerobic oxidation of trichloroethylene. Respectively, T_{50} and T_{90} for $LaCrO_3$ catalyst are reduced to about 50 and 20°C, compared with $LaMnO_3$. These results are in accordance with literature findings. For instance, Petrosious et al. [24] reported that chromium oxide exhibited higher activity in the degradation of chlorinated VOCs compared with oxides of manganese, iron, cobalt, nickel, and copper. Moreover, another study examined the activities of perovskite ABO_3 that included La, Y, Nd, and Gd in site-A and Co, Fe and Cr in B-site for oxidation of 1,2-dichlorobenzene in the presence or absence of water; the Cr-containing perovskites exhibited the uppermost catalytic activity despite having a smaller specific surface area compared to other perovskites [7]. From Figure 5, it is clear that the activity of the substituted catalyst $LaMn_{0.5}Cr_{0.5}O_3$ is superior to that of $LaCrO_3$ as well as $LaMnO_3$.

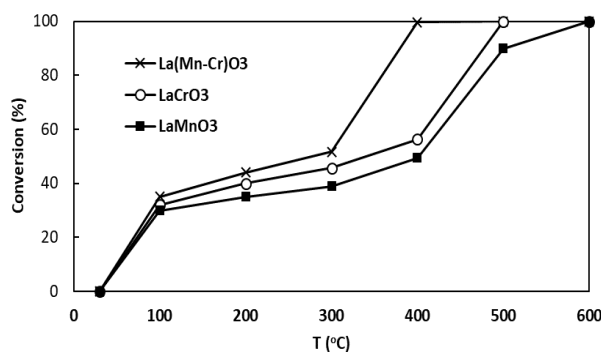**Fig. 5.** Catalytic oxidation of 1000 mg/l trichloroethylene in air by $LaMnO_3$, $LaCrO_3$, and $LaMn_{0.5}Cr_{0.5}O_3$ perovskites.

The associated T_{50} and T_{90} for the $LaMn_{0.5}Cr_{0.5}O_3$ catalyst were reduced to about 100 and 120°C, respectively, compared to the perovskite $LaMnO_3$ and about 50 and 100°C, respectively, compared to the $LaCrO_3$. The most important reason for this observation can be attributed to the higher specific surface area of the perovskite $LaMn_{0.5}Cr_{0.5}O_3$ (Table 1), as well as the relatively higher oxygen mobility (Figure 4) of this perovskite. These findings

are in accordance with the literature data regarding the catalytic performance of perovskites that were substituted in the B-position. Namely, it was reported that the activity of $LaMn_{0.6}Cu_{0.4}O_3$ was more active than that of $LaMnO_3$ and $LaCuO_3$ in the oxidation of carbon monoxide [13]. Moreover, $LaMn_{0.9}Fe_{0.1}O_3$ has higher activity compared to $LaMnO_3$ and $LaFeO_3$ in the oxidation of methane [25]. It is noteworthy that the substitution ratio is an important factor that influences the catalytic activity and the enhancement could not be seen on all the substitution ratios. The substituted catalyst in this study, namely $LaMn_{0.5}Cr_{0.5}O_3$ (50% Mn–50% Cr in site B), has the highest specific surface area and the highest mobility of oxygen, both of which can have a direct impact on catalytic activity. Most papers have shown that catalytic activity is directly related to these two factors. Spinicci et al. [26] investigated perovskite $LaBO_3$ (B=Mn, Co) for the oxidation of benzene. They concluded that $LaMnO_3$, with higher amount of surface oxygen species (based on the results of TPD analysis), showed higher activity. In another study, the perovskite $LaMn_{0.5}Co_{0.5}O_3$ showed the best results in the oxidation of CO due to high oxygen mobility. This reflects the fact that structural defects play an important role in improving oxygen mobility for perovskites [21]. Studying the combustion of chlorobenzene on the modified catalysts $LaMnO_3$, Lu et al. [27] concluded that the catalyst La-Sr-Mn, with the highest level of α oxygen, demonstrated the best catalytic activity. The XRD spectra of the $LaMnO_3$, $LaCrO_3$, and $LaMn_{0.5}Cr_{0.5}O_3$ samples after the oxidation reaction of 1000 mg/l trichloroethylene at the temperature range 25–600°C are provided in Figure 6. It is evident from the obtained XRD spectra that no discernible difference can be seen between the XRD patterns of the samples before (Figure 6a, b, and c) and after (Figure 6a', b', and c') the catalytic reaction. Thus, during the oxidation reaction, not only are no new phases are formed, but the perovskite phase is not destroyed. So, the crystalline phases of the perovskites remained intact during the oxidation reaction. The reason for this structure stability is that oxygen in the mixture of air and chlorinated VOCs can be adsorbed on the surface and directly participate in oxidation reaction or recover the extra oxygen of the perovskite. Thus, oxygen in the air plays an important role in maintaining the stability of the perovskite phase [14,28]. Sinquin et al. [6] observed that in the catalytic destruction of chlorinated C_2 compounds, $LaMnO_{3+\delta}$ is more stable than $LaCoO_3$. Due to having over-stoichiometric oxygen, the perovskite $LaMnO_{3+\delta}$ exhibited more structural stability than $LaCoO_3$.
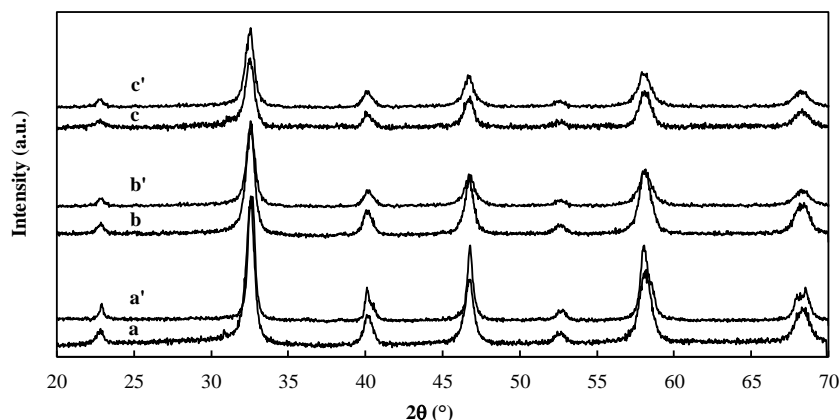
Fig. 6. XRD graph of perovskite (a) $LaMnO_3$, (b) $LaCrO_3$ and (c) $LaMn_{0.5}Cr_{0.5}O_3$ before and after (a', b', and c') oxidation reaction of 1000 mg/l trichloroethylene in air.

4. Conclusions

Employing the gel combustion method, the $LaMnO_3$, $LaCrO_3$, and $LaMn_{0.5}Cr_{0.5}O_3$ perovskite-type catalysts were elaborated. While the sole perovskite phases were observed in the XRD spectra of all the synthesized samples, other compounds such as oxides of manganese, chromium or lanthanum were not detected. The SEM images demonstrated that the perovskites possess a full spongy and porous structure, which is the dominant feature of the combustion method. The $LaMn_{0.5}Cr_{0.5}O_3$ sample had the highest BET specific surface area, which was equal to 26.8 m^2/g. Moreover, it showed the highest oxygen mobility as determined by O_2-TPD analysis. The order of catalytic activity of the probed perovskites for aerobic oxidation of 1000 mg/l of trichloroethylene in the air is $LaMn_{0.5}Cr_{0.5}O_3 > LaCrO_3 > LaMnO_3$. Moreover, due to the incorporation of these two metals in the substituted perovskite, T_{50} and T_{90} were reduced to about 100 and 120°C, respectively, as compared to $LaMnO_3$, as well as about 50 and 100°C, respectively, when compared to $LaCrO_3$.

References

[1] Li, W. B., Chu, W. B., Zhuang, M., Hua, J. (2004). Catalytic oxidation of toluene on Mn–containing mixed oxides prepared in reverse microemulsions. *Catalysis today*, *93*, 205-209.

[2] Li, W. B., Wang, J. X., Gong, H. (2009). Catalytic combustion of VOCs on non-noble metal catalysts. *Catalysis today*, *148*(1-2), 81–87.

[3] Sinquin, G., Petit, C., Hindermann, J. P., Kiennemann, A. (2001). Study of the formation of LaMO3 (M= Co, Mn) perovskites by propionates precursors: application to the catalytic destruction of chlorinated VOCs. *Catalysis today*, *70*(1-3), 183-196.

[4] Fu, Y. P., Hsu, C. S. (2005). Microwave-induced combustion synthesis of Li0. 5Fe2. 5– xMnxO4 powder

and their characterization. *Journal of alloys and compounds*, *391*(1-2), 185-189.

[5] Fino, D., Russo, N., Saracco, G., Specchia, V. (2007). Supported Pd-perovskite catalyst for CNG engines' exhaust gas treatment. *Progress in solid state chemistry*, *35*(2-4), 501-511.

[6] Sinquin, G., Petit, C., Libs, S., Hindermann, J. P., Kiennemann, A. (2001). Catalytic destruction of chlorinated C2 compounds on a LaMnO3+ δ perovskite catalyst. *Applied catalysis B: Environmental*, *32*(1-2), 37-47.

[7] Poplawski, K., Lichtenberger, J., Keil, F. J., Schnizlein, K., Amiridis, M. D. (2000). Catalytic oxidation of 1, 2-dichlorobenzene over ABO3-type perovskites. *Catalysis today*, *62*, 329–336.

[8] Van Roosmalen, J. A. M., Van Vlaanderen, P., Cordfunke, E. H. P. (1995). Phases in the Perovskite-Type LaMnO3+δ Solid Solution and the La2O3-Mn2O3 Phase Diagram. *Journal of Solid State Chemistry*, *114*, 516–523.

[9] Alagheband, R., Maghsoodi, S., Shahbazi Kootenaei A., Kianmanesh, H. (2018). Synthesis and Evaluation of ABO3 Perovskites (A=La and B=Mn, Co) with Stoichiometric and Overstoichiometric Ratios of B/A for Catalytic Oxidation of Trichloroethylene. *Bulletin of chemical reaction engineering and catalysis*, *13*, 47–56.

[10] Hartley, U. W., Tongnan, V., Laosiripojana, N., Kim-Lohsoontorn, P., Li, K. (2018). Nitrous oxide decomposition over La0.3Sr0.7Co0.7Fe0.3O3–δ catalyst. *Reaction Kinetics, mechanisms and catalysis*, *125*, 1–13.

[11] Abdolrahmani, M., Parvari, M., Habibpour, M. (2010). Effect of Copper Substitution and Preparation Methods on the LaMnO3±δ Structure and Catalysis of Methane Combustion and CO Oxidation. *Chinese journal of catalysis*, *31*, 394–403.

[12] Hou, Y., Ding, M., Liu, S., Wu, S., Lin, Y. (2014). Ni-substituted LaMnO3 perovskites for ethanol oxidation. *RSC advances*, *4*, 5329–5338.

[13] Pena, M. A., Fierro, J. L. G. (2001). Chemical Structures and Performance of Perovskite Oxides. *Chemical reviews*, *101*, 1981–2017.

[14] Maghsoodi, S., Towfighi, J., Khodadadi, A., Mortazavi, Y. (2013). The effects of excess manganese in nano-size lanthanum manganite perovskite on enhancement of trichloroethylene oxidation activity. *Chemical engineering journal*, *215-216*, 827–837.

[15] Prado-Gonjal, J., Arevalo-Lopez, A. M., Moran, E. (2011). Microwave-assisted synthesis: A fast and efficient route to produce $LaMO_3$ (M = Al, Cr, Mn, Fe, Co) perovskite materials. *Materials research bulletin*, *46*, 222–230.

[16] Ifrah, S., Kaddouri, A., Gelin, P., bergeret, G. (2007). On the effect of La–Cr–O– phase composition on diesel soot catalytic combustion. *Catalysis communications*, *8*, 2257–2262.

[17] Yu Ho, W., Hsun Hsu, Ch., Hua Tsia, M., Sen Yang, Y., Yung wang, D. (2010). Interlayer effect on the characterization of the La–Cr–O coatings with post-sputtering annealing treatment. *Applied surface science*, *256*, 2705–2710.

[18] Medkhali, A. H. A., Narasimharao, K., Basahel, S. N., Mokhtar, M. (2014). Divalent Transition Metals Substituted $LaFeO_3$ Perovskite Catalyst for Nitrous Oxide Decomposition. *Journal of membrane and separation technology*, *3*, 206–212.

[19] Álvarez-Galván, M. C., de la Peña O'Shea, V. A., Arzamendi, G., Pawelec, B., Gandıa, L. M., Fierro, J. L. G. (2009). Methyl ethyl ketone combustion over La-transition metal (Cr, Co, Ni, Mn) perovskites. *Applied catalysis B: Environmental*, *92*, 445–453.

[20] Shaterian, M., Enhessari, M., Rabbani, D., Asghari, M., Salavati-Niasari, M. (2014). Synthesis, characterization and photocatalytic activity of $LaMnO_3$ nanoparticles. *Applied surface science*, *318*, 213–217.

[21] Hosseini, S. A., Salari, D., Niaei, A., Arefi Oskoui, S. (2013). Physical–chemical property and activity evaluation of $LaB_{0.5}Co_{0.5}O_3$ (B = Cr, Mn, Cu) and $LaMn_xCo_{1-x}O_3$ (x = 0.1, 0.25, 0.5) nano perovskites in VOC combustion. *Journal of industrial and engineering chemistry*, *19*, 1903–1909.

[22] Ziaei-Azad, H., Khodadadi, A., Esmaeilnejad-Ahranjani, P., Mortazavi, Y. (2011). Effects of Pd on enhancement of oxidation activity of $LaBO_3$ (B = Mn, Fe, Co and Ni) perovskite catalysts for pollution abatement from natural gas fueled vehicles. *Applied catalysis B: Environmental*, *102*, 62–70.

[23] Windawi, H., Wyatt, M. (1993). Catalytic destruction of halogenated volatile organic compounds. *Platinum metals review*, *37*, 186–193.

[24] Petrosious, S. C., Drago, R. S., Young, V., Grunewald, G. C. (1993). Low-temperature decomposition of some halogenated hydrocarbons using metal oxide/porous carbon catalysts. *Journal of the american chemical society*, *115*, 6131–6137.

[25] Fino, D., Russo, N., Saracco, G., Specchia, V. (2007). Supported Pd-perovskite catalyst for CNG engines' exhaust gas treatment. *Progress in solid state chemistry*, *35*, 501–511.

[26] Spinicci, R., Faticanti, M., Marini, P., De Rossi, S., Porta, P. (2003). Catalytic activity of $LaMnO_3$ and $LaCoO_3$ perovskites towards VOCs combustion. *Journal of molecular catalysis A: Chemical*, *197*, 147–155.

[27] Lu, Y., Dai, Q., Wang, X. (2014). Catalytic combustion of chlorobenzene on modified $LaMnO_3$ catalysts. *Catalysis communications*, *54*, 114–117.

[28] Sinquin, G., Hindermann, J. P., Petit, C., Kiennemann, A. (1999). Perovskites as polyvalent catalysts for total destruction of C_1, C_2 and aromatic chlorinated volatile organic compounds. *Catalysis today*, *54*, 107–118.